Plant Physiol. (1986) 80, 863–869
0032-0889/86/80/0863/07/$01.00/0

Inorganic Carbon Uptake during Photosynthesis[1]

I. A THEORETICAL ANALYSIS USING THE ISOTOPIC DISEQUILIBRIUM TECHNIQUE

Received for publication October 2, 1985 and in revised form December 4, 1985

GEORGE S. ESPIE AND BRIAN COLMAN*
Department of Biology, York University, Downsview, Ontario, Canada M3J 1P3

ABSTRACT

Equations have been developed which quantitatively predict the theoretical time-course of photosynthetic ^{14}C incorporation when CO_2 or HCO_3^- serves as the sole source of exogenous inorganic carbon taken up for fixation by cells during steady state photosynthesis. Comparison between the shape of theoretical (CO_2 or HCO_3^-) and experimentally derived time-courses of ^{14}C incorporation permits the identification of the major species of inorganic carbon which crosses the plasmalemma of photosynthetic cells and facilitates the detection of any combined contribution of CO_2 and HCO_3^- transport to the supply of intracellular inorganic carbon. The ability to discriminate between CO_2 or HCO_3^- uptake relies upon monitoring changes in the intracellular specific activity (by ^{14}C fixation) which occur when the inorganic carbon, present in the suspending medium, is in a state of isotopic disequilibrium (JT Lehman 1978 J Phycol 14: 33–42). The presence of intracellular carbonic anhydrase or some other catalyst of the CO_2-HCO_3^- interconversion reaction is required for quantitatively accurate predictions. Analysis of equations describing the rate of ^{14}C incorporation provides two methods by which any contribution of HCO_3^- ions to net photosynthetic carbon uptake can be estimated.

A variety of experimental techniques, based on the slow interconversion between CO_2 and HCO_3^- (6), have recently been used to investigate DIC[2] transport in photosynthetic cells (12, 13, 18). These methods can be classified according to those which utilize a DIC system which is (a) approaching chemical equilibrium (18, 19) or (b) approaching isotopic equilibrium (1, 5, 7, 12). The third method (c) determines the maximum rate at which HCO_3^- dehydration provides CO_2 to a closed, aqueous system and compares this rate to the actual rate of photosynthesis (4, 13, 14). Experimentally, (c) is the simplest procedure and provides convincing evidence for HCO_3^- transport into cells if the photosynthetic rate greatly exceeds the CO_2 supply rate. However, application of this technique is limited to low DIC concentrations as the CO_2 supply rate is dependent on the DIC concentration (14).

From an analytical perspective, method (a) is complex in that the rate of photosynthesis and the concentration of $^{14}CO_2$ and $H^{14}CO_3^-$ continuously change during the time-course of the experiment. Detection of $H^{14}CO_3^-$ uptake is based upon a qualitative comparison of the shape of an experimental time-course of ^{14}C incorporation with those predicted for $^{14}CO_2$ or $H^{14}CO_3^-$ as the transported species (18). Alternatively, measurement of the rate of photosynthesis, following the addition of 'pure' $^{14}CO_2$ or $H^{14}CO_3^-$ to separate, DIC-depleted, cell suspensions, at a time when the concentration of $^{14}CO_2$ is momentarily equal in both suspensions, has also been used as a detection method (19). Bicarbonate transport is implied if the instantaneous rate of photosynthesis is higher when $H^{14}CO_3^-$ is supplied than when $^{14}CO_2$ is supplied (19).

Method (b), introduced by Lehman (12), reduces the analytical complexity associated with (a) without loss of resolution. In this modification, a trace quantity of $H^{14}CO_3^-$ is added to a cell suspension photosynthesizing at a constant rate such that the rate of photosynthesis, pH, and the bulk DIC concentration are not altered as a result of the addition. Under these conditions, changes which occur in the DIC system involve changes only in the SA of CO_2 and HCO_3^- (12). Since the value of SA_{CO_2} and $SA_{HCO_3^-}$ are distinctly different from one another during the approach to isotopic equilibrium, the shape of a ^{14}C incorporation time-course is characteristic of the species of DIC which permeates the cell and thus permits its identification.

Both methods (a) and (b) rely on the qualitative assessment of experimental results or upon the determination of the instantaneous rate of photosynthesis to identify the species of DIC which permeates the cells. In this paper, we extend the work of Lehman (12) by developing equations which quantitatively predict the theoretical time-course of ^{14}C incorporation, during steady state photosynthesis, when extracellular CO_2 or HCO_3^- serves as the sole source of DIC for photosynthesis. Direct comparison of theoretical and experimental curves permits the identification of the major species of DIC taken up by photosynthetic cells and facilitates detection of any combined uptake of CO_2 and HCO_3^-. A method is also described whereby the apparent rate constant of isotopic equilibrium can be estimated from ^{14}C incorporation data. This procedure affords the opportunity to assess the influence of extracellular factors on the uptake of DIC and to estimate the contribution of HCO_3^- uptake to the intracellular supply of DIC.

BACKGROUND AND DERIVATION OF BASIC EQUATIONS[3]

The chemical reactions

$$CO_2 + H_2O \underset{k_{-1}}{\overset{k_1}{\rightleftharpoons}} H^+ + HCO_3^- \quad (1)$$

and

$$CO_2 + OH^- \underset{k_{-3}}{\overset{k_3}{\rightleftharpoons}} HCO_3^- \quad (2)$$

[1] Supported by grants from the Natural Sciences and Engineering Research Council of Canada (NSERC). G. S. E. is the recipient of an NSERC Postgraduate Scholarship.

[2] Abbreviations: DIC, dissolved inorganic carbon; CA, carbonic anhydrase; dpm, disintegrations per minute; SA, specific activity.

[3] We have used the original notation of Lehman (12) where practical.

govern the kinetics of the interconversion among CO_2, HCO_3^-, and CO_3^{2-} as the reaction

$$HCO_3^- \rightleftharpoons H^+ + CO_3^{2-} \quad (3)$$

is virtually instantaneous (16). The rate constants, k_1, k_{-1}, k_3 and k_{-3}, are related to the equilibrium constant, K_{a1}, of reaction (1) by the equations

$$K_{a1} = \frac{k_1}{k_{-1}} = \frac{[H^+][HCO_3^-]}{[CO_2]} \quad (4)$$

and

$$\frac{K_{a1}}{K_w} = \frac{k_3}{k_{-3}} = \frac{[HCO_3^-]}{[CO_2][OH^-]} \quad (5)$$

where

$$K_w = [H^+][OH^-]$$

The numerical values of the rate constants, at 25°C and infinite dilution are $k_1 = 0.037\ s^{-1}$ and $k_3 = 8500\ M^{-1}\ s^{-1}$ (15). At other temperatures we have used the equations

$$\log k_1 = -\frac{3900}{T} + 11.59 \quad (7)$$

and

$$\log k_3 = -\frac{2897}{T} + 13.65 \quad (8)$$

to determine the rate constants. Equations 7 and 8 are derived from the data given by Kern (11) and T is in degrees Kelvin. Values for the equilibrium constants K_{a1} and K_{a2} (Eq. 3) are given by Harned *et al.* (9, 10) and at 25°C are 4.45×10^{-7} M and 4.69×10^{-11} M, respectively.

The value of K_w is taken as $1.01 \times 10^{-14}\ M^2$ (17). The equilibrium concentrations of CO_2, HCO_3^- and CO_3^{2-} in solution of constant DIC concentration and pH were calculated from the equations of Buch (2).

Isotopic Disequilibrium. From a consideration of the rate equations describing the interconversion between CO_2 and HCO_3^-, Lehman (12) has shown that the formation of $^{14}CO_2$ from $H^{14}CO_3^-$, added to a solution of constant pH and temperature, follows the equation

$$[^{14}CO_2] = (1 - e^{-\alpha_1 t})\frac{\beta_1}{\alpha_1}. \quad (9)$$

Similarly, it can also be shown (3) that the disappearance of $H^{14}CO_3^-$ follows the equation

$$[H^{14}CO_3^-] = \left([H^{14}CO_3^-]_0 - \frac{\beta_2}{\alpha_2}\right)e^{-\alpha_2 t} + \frac{\beta_2}{\alpha_2}. \quad (10)$$

The terms α and β are constants and equations relating these terms to the rate and equilibrium constants of reactions (1 to 3) are given in Table I. The ratios β_1/α_1 and β_2/α_2 represent the equilibrium concentrations of $^{14}CO_2$ and $H^{14}CO_3^-$, respectively. The expression $[H^{14}CO_3^-]_0 - \beta_2/\alpha_2$ is the total change in $H^{14}CO_3^-$ concentration (*i.e.* $\Delta H^{14}CO_3^-$), where $[H^{14}CO_3^-]_0$ is the concentration at $t = 0$ (seconds). For the situation in which $H^{14}CO_3^-$ is is added, to initiate isotopic disequilibrium, $\Delta[^{14}CO_2]$ is equal to β_1/α_1, as $[^{14}CO_2]_0$ is zero.

If $H^{14}CO_3^-$ (or $^{14}CO_2$) is added to a solution containing a relative excess of unlabeled DIC, such that the DIC system remains at or close to chemical equilibrium, then changes only in the SA of the various DIC species occur (12). Initially, the values of SA_{CO_2} and $SA_{HCO_3^-}$ are distinctly different, but, as the exchange reactions progress, the values exponentially approach a common value, SA_{DIC}, which is the SA of the bulk DIC system. The value of SA_{DIC}, however, does not change during the approach to isotopic equilibrium as total radioactivity and DIC are conserved. In this context, SA_{DIC} is analogous to β_1/α_1 or β_2/α_2, *i.e.* it represents the equilibrium being approached by the system. However, the exponential terms of Eqs. 9 and 10 govern the rate at which isotopic equilibrium is achieved. Substituting SA_{DIC} into Eqs. 9 and 10, to solve for SA_{CO_2} and $SA_{HCO_3^-}$, yields, upon rearrangement,

$$SA^B_{CO_2} = SA^B_{DIC}(1 - e^{-\alpha_1 t}) \quad (19)$$

and

$$SA^B_{HCO_3^-} = \Delta SA^B_{HCO_3^-} \cdot \left(\frac{SA^B_{DIC}}{\Delta SA^B_{HCO_3}} + e^{-\alpha_2 t}\right). \quad (20)$$

The superscript B (or C, Table II) refers to the radiochemical species of $DI^{14}C$ used to initiate isotopic equilibrium (*i.e.* $H^{14}CO_3^-$ or $^{14}CO_2$) and the subscripts CO_2 and HCO_3^- indicate the particular DIC species for which the specific activity is calculated.

Photosynthetic ^{14}C Incorporation. During steady state photosynthesis in a medium of fixed DIC concentration, SA and pH, the rate of ^{14}C incorporation by cells is constant and described by the equation

$$\frac{d\,(dpm)}{dt} = V = PS \cdot Chl \cdot SA_{DIC} \cdot 2.22 \times 10^6/3600. \quad (21)$$

The incorporation velocity, V, is given in units of $dpm \cdot s^{-1}$. PS is the rate of photosynthesis ($\mu mol\ C \cdot mg^{-1}Chl \cdot h^{-1}$), Chl is the quantity of chlorophyll per sample (mg), and SA_{DIC} is the specific activity ($\mu Ci \cdot \mu mol^{-1}$). The constants 2.22×10^6 ($dpm \cdot \mu Ci^{-1}$) and 3600 ($s \cdot h^{-1}$) are required to obtain the appropriate units. The radioactivity (dpm) incorporated at any given time is predicted by the integrated form of Eq. 21 and is simply

$$dpm_t = V \cdot t. \quad (22)$$

The specific activities of the components of the DIC system are not constant for cells which experience a transient isotopic disequilibrium, but change according to Eqs. 19 and 20. If we assume that CO_2 alone is taken up by the cells and that the intracellular specific activity (SA_i) is equal to $SA^B_{CO_2}$ (Eq. 19),

Table I. *Summary of Equations*[a]

g	$= (k_1 + k_3 \cdot K_w/[H^+])$	(11)
h	$= k_1\,[H^+]/K_{a1} + k_3 K_w/K_{a1}$	(12)
[DIC]	$= [CO_2] + [HCO_3^-] + [CO_3^{2-}]$	(13)
C_b	$= [HCO_3^-]/([HCO_3^-] + [CO_3^{2-}])$	(14)
α_1	$= g + hC_b$	(15)
β_1	$= hC_b[DIC]$	(16)
α_2	$= g/C_b + h$	(17)
β_2	$= g[DIC]$	(18)

[a] After Lehman (12)

Table II. *Summary of Equations*

Equations used to calculate the specific activity of CO_2 and HCO_3^- in solution, the theoretical rate of ^{14}C incorporation and time-course of ^{14}C incorporation by photosynthetic cells, following the initiation of isotopic disequilibrium by $H^{14}CO_3^-$ or $^{14}CO_2$ addition. Equations based on assumption that CO_2 or HCO_3^- alone is taken up by photosynthetic cells.

$H^{14}CO_3^-$ ADDITION		$^{14}CO_2$ ADDITION	
SPECIFIC ACTIVITY			
$SA^B_{CO_2} = SA_{DIC}(1 - e^{-\alpha_1 t})$	(19)	$SA^C_{CO_2} = \Delta SA^C_{CO_2}\left(\frac{SA^C_{DIC}}{\Delta SA^C_{CO_2}} + e^{-\alpha_1 t}\right)$	(32)
$SA^B_{HCO_3^-} = \Delta SA^B_{HCO_3^-}\left(\frac{SA^B_{DIC}}{\Delta SA^B_{HCO_3^-}} + e^{-\alpha_2 t}\right)$	(20)	$SA^C_{HCO_3^-} = SA^C_{DIC}(1 - e^{-\alpha_2 t})$	(33)
RATE OF ^{14}C-INCORPORATION -- CO_2 UPTAKE			
$\frac{d(DPM)}{dt} = V^B_{CO_2}(1 - e^{-\alpha_1 t})$	(27)	$\frac{d(DPM)}{dt} = V^C_{CO_2}\left(\frac{SA^C_{DIC}}{\Delta SA^C_{CO_2}} + e^{-\alpha_1 t}\right)$	(34)
$V^B_{CO_2} = 616.67 \cdot PS \cdot Chl \cdot SA^B_{DIC}$	(28)	$V^C_{CO_2} = 616.67 \cdot PS \cdot Chl \cdot \Delta SA^C_{CO_2}$	(35)
RATE OF ^{14}C-INCORPORATION -- HCO_3^- UPTAKE			
$\frac{d(DPM)}{dt} = V^B_{HCO_3^-}\left(\frac{SA^B_{DIC}}{\Delta SA^B_{HCO_3^-}} + e^{-\alpha_2 t}\right)$	(29)	$\frac{d(DPM)}{dt} = V^C_{HCO_3^-}(1 - e^{-\alpha_2 t})$	(36)
$V^B_{HCO_3^-} = 616.67 \cdot PS \cdot Chl \cdot \Delta SA^B_{HCO_3^-}$	(30)	$V^C_{HCO_3^-} = 616.67 \cdot PS \cdot Chl \cdot SA^C_{DIC}$	(37)
^{14}C-INCORPORATION -- CO_2 UPTAKE			
$DPM_t = \frac{V^B_{CO_2}}{\alpha_1}(e^{-\alpha_1 t} + \alpha_1 t - 1)$	(26)	$DPM_t = \frac{V^C_{CO_2}}{\alpha_1}\left(-e^{-\alpha_1 t} + \frac{\alpha_1 SA^C_{DIC}\, t}{\Delta SA^C_{CO_2}} + 1\right)$	(38)
^{14}C-INCORPORATION -- HCO_3^- UPTAKE			
$DPM_t = \frac{V^B_{HCO_3^-}}{\alpha_2}\left(-e^{-\alpha_2 t} + \frac{\alpha_2 SA^B_{DIC}\, t}{\Delta SA^B_{HCO_3^-}} + 1\right)$	(31)	$DPM_t = \frac{V^C_{HCO_3^-}}{\alpha_2}(e^{-\alpha_2 t} + \alpha_2 t - 1)$	(39)

then the rate of change of ^{14}C incorporation is given by

$$\frac{d(\text{dpm})}{dt} = 616.67 \cdot PS \cdot Chl \cdot SA^B_{CO_2} \quad (23)$$

$$= 616.67 \cdot PS \cdot Chl \cdot SA^B_{DIC}(1 - e^{-\alpha_1 t}) \quad (24)$$

$$= V^B_{CO_2}(1 - e^{-\alpha_1 t}) \quad (25)$$

when $H^{14}CO_3^-$ is employed to initiate isotopic disequilibrium.

The assumption used in developing Eq. 25 effectively requires that the exchange flux of CO_2 between the cells and the surrounding medium occurs rapidly with respect to the change of $SA^B_{CO_2}$. This assumption can be tested experimentally by following the time-course of ^{14}C incorporation when CA is included in the cell suspension. In this case, isotopic equilibrium is attained within a few milliseconds and, since the rate of photosynthesis is constant, fixation of ^{14}C will be a linear function of time (*i.e.* $SA_i = SA_{DIC}$), if the intracellular pool turns over rapidly. Alternatively, if the value of SA_i gradually approaches the value of SA_{DIC} (slow turnover), then a lag in ^{14}C incorporation is expected and the extrapolated value of the *y*-intercept, from the linear portion of a ^{14}C incorporation *versus* time plot, will be negative.

The incorporation of ^{14}C into products of photosynthesis (−CA) is predicted by the integrated form of Eq. 25 and is, following rearrangement,

$$\text{dpm}_t = \frac{V^B_{CO_2}}{\alpha_1}(e^{-\alpha_1 t} + \alpha_1 t - 1). \quad (26)$$

Using similar considerations, equations for the HCO_3^- component of SA can also be derived (Table II). These equations quantitatively predict the time-course of ^{14}C incorporation assuming that CO_2 or HCO_3^- alone is taken up. Isotopic disequilibrium can also be initiated by the addition of a small quantity of $^{14}CO_2$. Equations for this case are summarized in Table II.

RESULTS AND DISCUSSION

Effect of Temperature and pH. The temperature and pH dependence of the approach to isotopic equilibrium ($t_{1/2}$), at low ionic strength, are given in Figure 1. Equilibrium is established most slowly at low temperature and pH 7.5 (12), requiring more than 90 s for 50% completion at 10°C. At pH values below 7.5, the contribution of reaction (2) to establishing equilibrium is minimal, while the velocity of the dehydration reaction (1) is enhanced by increasing H^+ concentration. Consequently, $t_{1/2}$ decreases with decreasing pH (Fig. 1). Above pH 7.5, both reactions (1) and (2) contribute to establishing equilibrium, the significance of reaction (2) increasing with pH.

Specific Activity of the DIC Component. Figure 2 (pH 7.5, 25°C) illustrates the expected changes in the SA of the DIC components for the situations where isotopic disequilibrium is initiated by $H^{14}CO_3^-$ or $^{14}CO_2$ addition. The conditions (Fig. 2) are adjusted so that $SA^B_{HCO_3^-}$ ($H^{14}CO_3^-$ addition) and $SA^C_{CO_2}$

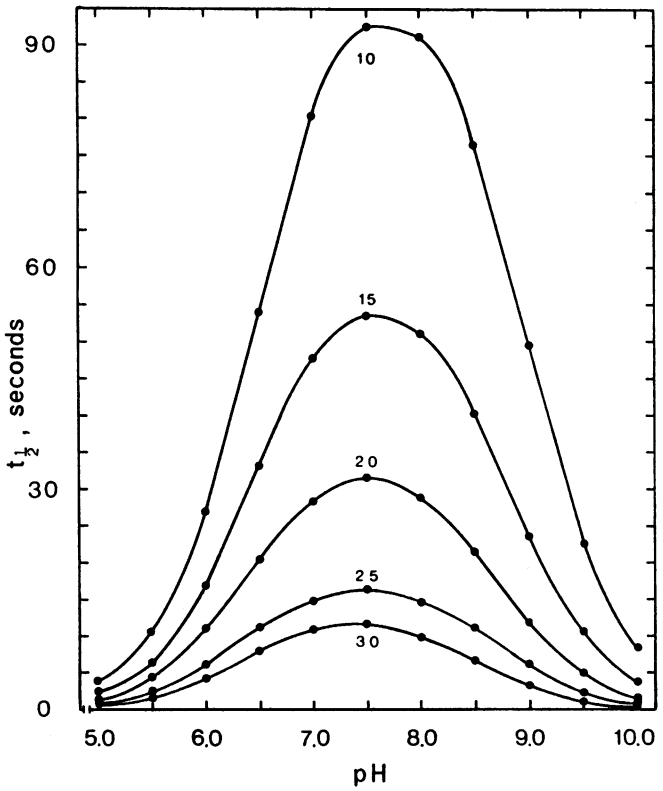

FIG. 1. The pH and temperature dependence of the approach to one-half isotopic equilibrium ($t_{½}$). Temperatures are in °C.

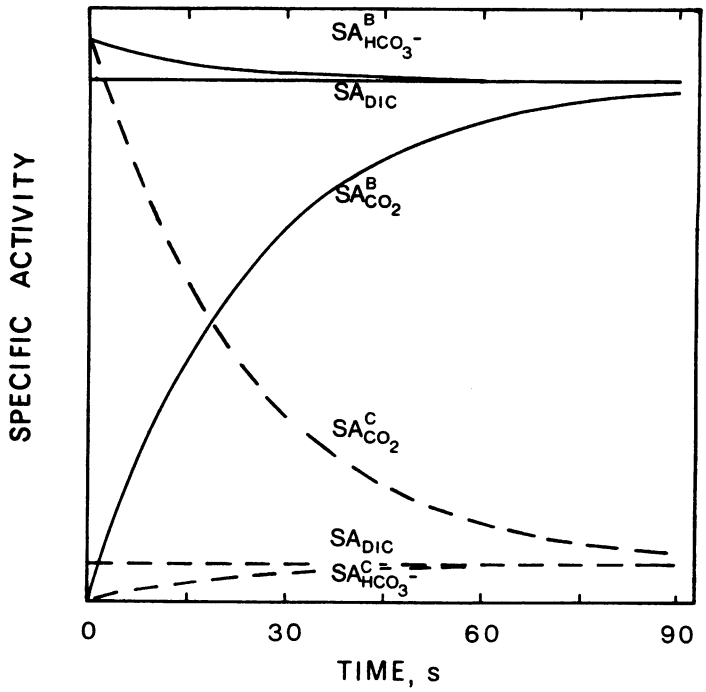

FIG. 2. Time-dependent changes in the specific activity of CO_2 and HCO_3^- (as labeled) following the initiation of isotopic disequilibrium by $H^{14}CO_3^-$ (——) addition or $^{14}CO_2$ (– – –) addition in a closed aqueous system containing an equilibrium distribution of $H^{12}CO_3^-$ and $^{12}CO_2$. Initial conditions have been adjusted such that $SA^B_{HCO_3^-}$ ($H^{14}CO_3^-$ addition) equals $SA^C_{CO_2}$ ($^{14}CO_2$ addition). Lines marked DIC represent the specific activity of the inorganic carbon system as a whole. The curves were calculated from the equations given in Table II for 25°C and pH 7.5.

[$^{14}CO_2$ addition) are initially equal. In the case of $H^{14}CO_3^-$ addition, $SA^B_{CO_2}$ is initially zero, but increases with time, approaching the equilibrium value SA^B_{DIC}, over a period of more than 90 s (Fig. 2). The change in $SA^B_{HCO_3^-}$ is small in this particular case (pH 7.5) as chemical equilibrium greatly favors HCO_3^-.

The value of SA_{DIC} remains constant if total radioactivity and DIC are conserved, but the absolute values differ in the two cases as a consequence of the initial criterion [$SA^B_{HCO_3^-} = SA^C_{CO_2}$]. Maintaining SA_{DIC} constant for $H^{14}CO_3^-$ and $^{14}CO_2$ addition is also an acceptable procedure; however, care must be exercised to ensure that chemical equilibrium is not significantly disturbed when pH of the solution is far from the apparent pK_{a1} of H_2CO_3 (6.35 at 25°C).

The change in SAs occurs in an opposite direction to that described above when $^{14}CO_2$ is used to initiate isotopic disequilibrium (Fig. 2). $SA^C_{CO_2}$ declines in value while a small increase in $SA^C_{HCO_3^-}$ occurs (Fig. 2). Again, both components approach equilibrium over a time period in excess of 90 s.

Photosynthetic ^{14}C Incorporation during Isotopic Disequilibrium. The theoretical time-courses of ^{14}C incorporation by photosynthetic cells, which experience a transient isotopic disequilibrium, are given in Figure 3. These curves were calculated using the equations given in Table II. Equation 22 was used to calculate the lines marked +CA since isotopic equilibrium is achieved very rapidly in the presence of this enzyme.

A distinct lag in the incorporation of ^{14}C is predicted ($H^{14}CO_3^-$ addition) if the cells take up CO_2 alone (Fig. 3). The incorporation of ^{14}C eventually becomes a linear function of time as isotopic equilibrium is achieved. Alternatively, the uptake of HCO_3^- by the cells would result in an almost constant rate of ^{14}C incorporation, as the change in $SA_{HCO_3^-}$ is small. In the presence of extracellular CA, incorporation of ^{14}C (taken up as $^{14}CO_2$ or $H^{14}CO_3$) is expected to be slightly less than that predicted for cells which utilize HCO_3^- (+CA, Fig. 3).

When isotopic disequilibrium is initiated by the addition of $^{14}CO_2$, an initial rapid incorporation of ^{14}C is predicted, if CO_2 is the sole source of DIC taken up. The rate of ^{14}C incorporation declines over time becoming constant as equilibrium is attained. If HCO_3^- alone is taken up, however, a small lag in ^{14}C incorporation is anticipated. This time photosynthetic ^{14}C incorporation is expected to be slightly less than that predicted when extracellular CA is included in the reaction medium (Fig. 3).

Figure 4 shows the pH dependence of the expected patterns of ^{14}C incorporation for CO_2 or HCO_3^- uptake alone. Since isotopic equilibrium is established most slowly at pH 7.5 (Fig. 1) (12), the duration of the nonlinear portion of the time-course plots is expected to be a maximum at this pH, as is evident in Figure 4, A and B (CO_2 uptake). This is, however, not obvious from Figure 4, C and D (HCO_3^- uptake). Although it can be shown by calculation that the duration of the nonlinear portion of the time-course plots is in fact a maximum at this pH, the degree of curvature is very slight. The duration and degree of curvature are controlled by two factors: the time required to establish isotopic equilibrium and the magnitude of the change in $SA_{HCO_3^-}$ or SA_{CO_2}. As the pH of the medium is increased or decreased around 7.5, the duration of the nonlinear portion of the time-course plots decreases. However, the magnitude of the change in $SA_{HCO_3^-}$ increases under acidic conditions, whereas the magnitude of the change in SA_{CO_2} increases under alkaline conditions. The net effect created by the interaction of these factors is that the most pronounced curvatures occur around pH 6.3 (Fig. 4, C and D) or pH 7.5 (Fig. 4, A and B). Thus, by the appropriate manipulation of pH (and temperature), significantly different predictions arise which may be utilized to investigate inorganic carbon transport.

Effect of CO_2 plus HCO_3^- Transport on SA_i and Photosynthetic ^{14}C Incorporation. Lipid bilayers are far more permeable

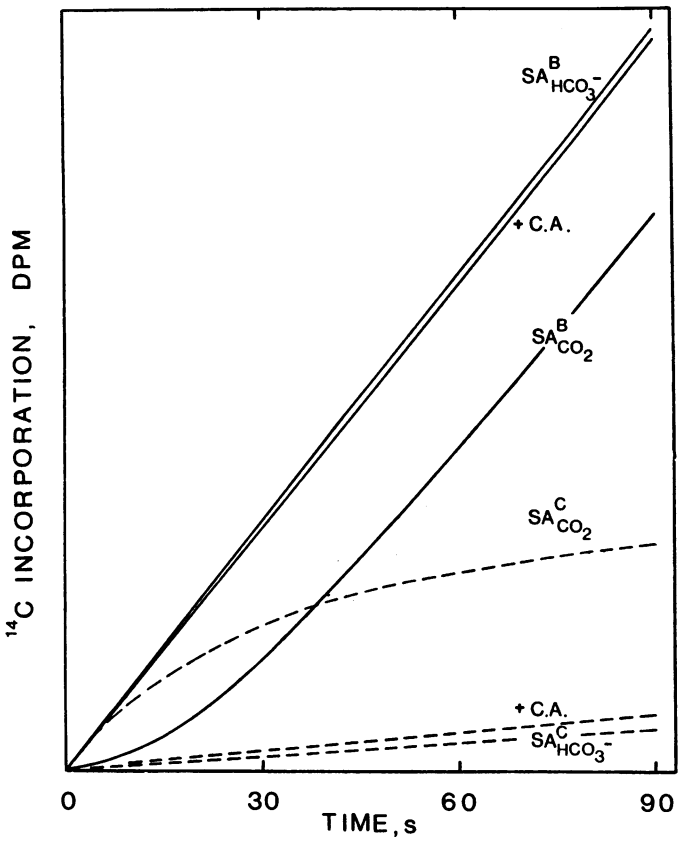

FIG. 3. Theoretical time-course of photosynthetic ^{14}C incorporation by cells which experience a transient isotopic disequilibrium, initiated by $H^{14}CO_3^-$ (——) addition or $^{14}CO_2$ (- - -). The curves were calculated from the equations given in Table II, assuming that the intracellular specific activity is equal to either the specific activity of CO_2 or HCO_3^- (as labeled) in the suspending medium (pH 7.5, 25°C). Also shown are the expected time-courses of ^{14}C incorporation when isotopic equilibrium is attained instantaneously (+CA). In all cases the rate of photosynthesis is constant.

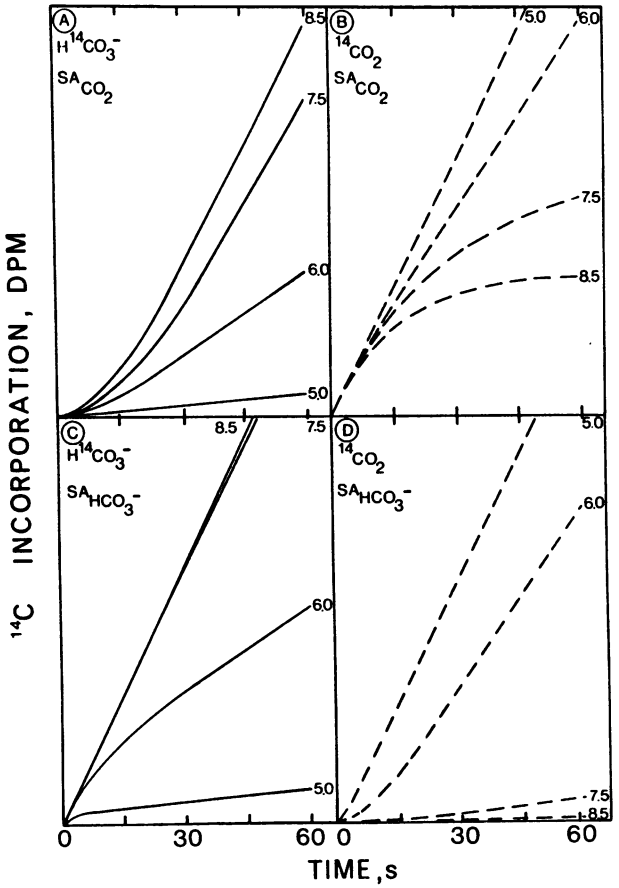

FIG. 4. The effect of pH (labeled at right) upon the theoretical time-course of photosynthetic ^{14}C incorporation, during the approach to isotopic equilibrium, following $H^{14}CO_3^-$ (——) addition or $^{14}CO_2$ (- - -) addition. The specific activity of the particular DIC species used in the calculations is labeled in the upper left-hand corner of each panel. Initially, $SA^B_{CO_2}$ ($H^{14}CO_3^-$ additions) equals $SA^C_{CO_2}$ ($^{14}CO_2$) addition). In all cases the rate of photosynthesis is constant and calculations are based on the same numerical value of this rate at 25°C. All values of dpm are plotted on the same scale.

to CO_2 than to HCO_3^- (8). Passive flux of HCO_3^- into photosynthetic cells is, therefore, expected to be minimal. However, the exchange between intracellular and extracellular CO_2 and net influx of CO_2, following a concentration gradient, encounters substantially less resistance. In this case, changes in the intracellular specific activity (SA_i), during isotopic disequilibrium, should closely follow the changes in SA_{CO_2}. If carrier-mediated HCO_3^- transport occurs, its contribution of ^{14}C to the intracellular DIC pool is in addition to that provided by CO_2 exchange. Consequently, the value of SA_i is expected to be intermediate between that predicted for CO_2 or HCO_3^- uptake. A quantitatively different time-course of ^{14}C incorporation is, therefore, expected if both CO_2 and HCO_3^- transport contribute to the intracellular supply of DIC, as the value of SA_i governs the ratio of $^{14}C/^{12}C$ fixation. Observable differences in an experimental time-course would be manifested as a change in the degree and duration of the nonlinear portion of the fixation curve as well as increased incorporation of ^{14}C compared to that predicted for CO_2 uptake alone (Figs. 3, 4).

Estimating the Contribution of HCO_3^- to Net DIC Uptake. At equilibrium, the value of $e^{-\alpha_1 t}$ is zero and ^{14}C incorporation becomes a linear function of time. Using equation (26) ($H^{14}CO_3^-$ addition) as an example, the straight line portion of the time-course is described by

$$\mathrm{dpm}_t = V^B_{CO_2} \cdot t - \frac{V^B_{CO_2}}{\alpha_1} \tag{40}$$

where $V^B_{CO_2}$ is the slope of the line and $V^B_{CO_2}/\alpha_1$ is the y-intercept. Provided the rate of photosynthesis and pH remain constant, the slope of the ^{14}C incorporation time-course will be the same, regardless of whether HCO_3^- is taken up by the cells or not, since the SA of the DIC species are equal at equilibrium. However, uptake of HCO_3^- results in an SA_i which is higher in value than that predicted for CO_2 uptake alone. Consequently, ^{14}C incorporation will be higher than predicted, thereby displacing the linear portion of the ^{14}C fixation time-course upward. In this event, the value of the y-intercept changes and the difference between the actual and predicted intercepts ($b_o - b_p$) represents ^{14}C incorporation which cannot be accounted for on the basis of CO_2 uptake alone. In other words, the ^{14}C incorporation in excess of the maximum possible contribution of ^{14}C from CO_2 uptake must be attributed to ^{14}C taken up from the medium as $H^{14}CO_3^-$. The contribution of $H^{14}CO_3^-$ ions (B), expressed as a percentage of the theoretical net $DI^{14}C$ uptake arising from photosynthetic consumption, is

$$B = \frac{b_o - b_p}{\mathrm{dpm}_{t(eq)}} \times 100 \tag{41}$$

where $\mathrm{dpm}_{t(eq)}$ is the predicted incorporation of ^{14}C at the time that isotopic equilibrium is attained. For the purpose of this estimate, the right hand side of this Eq. 40 is used to determine

$dpm_{t(eq)}$ and $t(eq)$ is approximated as, 99.99% of isotopic equilibrium, from the expression $\ln 0.01/-\alpha_1$.

From a practical point of view, this method, of estimating the contribution of HCO_3^- ions requires that the sampling of cell suspensions be extended well into the equilibrium phase of the time-course, in order to accurately estimate the slope and y-intercept. However, prolonged photosynthesis may substantially reduce the DIC concentration, possibly resulting in a decrease in the rate of photosynthesis and in a change in the slope and y-intercept. For this reason, the application of this method must be restricted to situations where the DIC concentration is well above the saturation level.

Examination of Eq. 40, however, suggests an alternative approach. The y-intercept, $V^B_{CO_2}/\alpha_1$, is defined by the slope, $V^B_{CO_2}$, and α_1, which is the overall rate constant of equilibration. In any given experiment, the slopes of observed and predicted time-courses (linear portion) are identical and, consequently, the y-intercept will be uniquely defined by the apparent value of α_1. In other words, HCO_3^- transport will be manifested as an apparent change in the value of α_1, but this is not to say that the actual rate of exchange between CO_2 and HCO_3^- (in the medium) is altered. An apparent change in the value of α_1 is the consequence of intracellular DIC being acquired from two external sources, CO_2 and HCO_3^-. The ^{14}C incorporation time-course merely indicates the value of SA_i at any given time. It does not strictly monitor the progress of the interconversion reactions towards equilibrium, although this would be the case if only CO_2 or HCO_3^- were taken up. Thus, an apparent change in the value of α_1 means that acquisition of intracellular ^{14}C is not rigidly controlled by the kinetics of the interconversion reactions and indicates the involvement of HCO_3^- transport. Substituting the terms $-V^B_{CO_2}/\alpha_{ob}$ and $-V^B_{CO_2}/\alpha_1$ for b_o and b_p in Eq. 41 together with the right-hand side of Eq. 40 for the term $dpm_{t(eq)}$, will also yield an expression describing the fractional contribution of $H^{14}CO_3^-$ ions and is, following rearrangement,

$$B = \frac{\alpha_{ob} - \alpha_1}{\alpha_{ob} \cdot \alpha_1 \cdot t_{(eq)} - \alpha_{ob}}. \quad (42)$$

The experimental value of a (α_{ob}) and $V^B_{CO_2}$ can be estimated by nonlinear regression analysis using average rates of ^{14}C incorporation, calculated from a time-course experiment, and time as the input variables. The average rate of ^{14}C incorporation is determined, over small time intervals, as the slope of the line between two consecutive data points. The theoretical nonlinear regression model, for this example, is given by Eq. 25 and predicts the rate of ^{14}C incorporation as a function of time, if CO_2 alone is taken up ($H^{14}CO_3^-$ addition). The expected shapes of rate *versus* time plots are identical to those shown for the dependence of SA on time (Fig. 2). This method provides a sensitive means by which a small deviation from the theoretical expectation can be detected, as the analysis employs the entire observed trend of the rate of ^{14}C incorporation to arrive at estimates of α_{ob} and $V^B_{CO_2}$.

If SA_i equals $SA^B_{CO_2}$ at all times during isotopic disequilibrium, then the predicted values of $V^B_{CO_2}$ and α_1 will satisfy the observations, and the ratio of α_{ob}/α_1 will be unity. When SA_i takes on values which are somewhat higher than predicted by $SA^B_{CO_2}$ (*i.e.* HCO_3^- uptake), incorporation of ^{14}C will occur at faster rates than can be reconciled by the kinetics of the interconversion reactions, and the ratio α_{ob}/α_1 will be greater than unity. Within the limits of experimental error, however, the observed and predicted values of $V^B_{CO_2}$ will, of necessity, be equal as $V^B_{CO_2}$ depends only on the maintenance of a constant rate of photosynthesis and the equilibrium value of SA_{DIC}. The necessary equivalence of observed and predicted values of $V^B_{CO_2}$ can, therefore, provide a valuable internal check of prior calculations and the validity of experimental results.

The possibility arises that α_{ob}/α_1 may be less than unity, indicating that SA_i is less than $SA^B_{CO_2}$ during the approach to isotopic equilibrium. The exchange flux of CO_2 between the cells and the medium cannot then be assumed to occur instantaneously. A contribution of HCO_3^- ions to net DIC uptake cannot be conclusively ruled out in this event, but diffusion limited uptake of CO_2 alone is adequate to explain this observation.

A Requirement for Intracellular CA. An assumption implicit in the calculations described is that the intracellular specific activity of CO_2 and HCO_3^- are maintained in instantaneous equilibrium with respect to each other and the transported DIC species, while the extracellular DIC approaches isotopic equilibrium. This condition is necessary to ensure that the availability of the $DI^{14}C$ substrate fixed in the primary carboxylation reaction is not limited by a slow interconversion between CO_2 and HCO_3^- within the cells. If this is the situation, however, the results of isotopic disequilibrium experiments will reflect this limitation in ^{14}C-substrate. Thus, the presence of intracellular CA, or some other catalyst of the interconversion reaction, is required to enhance the intracellular rate of reaction.

Conclusion. The equations developed here provide a means by which the incorporation of ^{14}C by photosynthetic cells can be quantitatively predicted when CO_2 or HCO_3^- serves as the sole source of DIC available for uptake during steady state photosynthesis. The present analysis, therefore, establishes valuable baseline criteria from which to assess the role that CO_2 or HCO_3^- uptake plays in the supply of intracellular DIC, for photosynthesis. This scheme differs from other methods (7, 18) in that the ability to discriminate between CO_2 or HCO_3^- uptake relies upon monitoring the changes in SA_i (by ^{14}C fixation) which occur during isotopic disequilibrium, rather than upon the assumption that ^{14}C fixation is linearly proportional to $^{14}CO_2$ or $H^{14}CO_3^-$ concentration. The latter assumption is only valid when the concentration of DIC is low (6, 18), and thus quantitative evaluation of experimental data must be confined within a small DIC concentration range. Since the overall rate constant of isotopic equilibration (α) is independent of CO_2 and HCO_3^- concentration, the application of the isotopic disequilibrium procedure need not be restricted to low DIC concentrations but can be employed quantitatively over a wide range of concentrations. In an accompanying paper we demonstrate the utility of the present scheme in evaluating the uptake of DIC by photosynthetically active *Asparagus* mesophyll cells.

Acknowledgments.—We would like to express our appreciation to Darlene Ager, John Cats, John Fox, and Robert H. Haynes for providing valuable advice and assistance and Ms. Despy Whyte-Simms for patiently typing the manuscript.

LITERATURE CITED

1. BADGER MR, TJ ANDREWS 1982 Photosynthesis and inorganic carbon usage by the marine cyanobacterium, *Synechococcus* sp. Plant Physiol 70: 517–523
2. BUCH K 1960 Dissoziation der Kohlensaure, Gleichgewicht und Puffersysteme. *In* W Ruhland, ed, Handbuch der Pflanzenphysiologie, Vol 1. Springer-Verlag, Berlin, pp 1–11
3. ESPIE GS 1985 Photosynthesis and the mechanism of inorganic carbon acquisition in isolated *Asparagus* mesophyll cells and other photosynthetic cells. PhD thesis. York University, Toronto
4. ESPIE GS, B COLMAN 1982 Photosynthesis and inorganic carbon transport in isolated *Asparagus* mesophyll cells. Plant Physiol 70: 649–654
5. ESPIE GS, GW OWTTRIM, B COLMAN 1984 A comparative study of inorganic carbon transport in photosynthetic cells. *In* C Sybesma, ed, Advances in Photosynthesis Research, Vol 3. Martinus Nijoff/Dr. W Junk Publishers, The Hague, pp 681–684
6. FILMER DL, TG COOPER 1970 Effect of varying temperature and pH upon the predicted rate of "CO_2" utilization by carboxylases. J Theor Biol 29: 131–145
7. FINDENEGG GR 1980 Inorganic carbon transport in microalgae. II. Uptake of HCO_3^- ions during photosynthesis of five microalgal species. Plant Sci Lett 18: 289–297
8. GUTKNECHT J, MA BISSON, FC TOSTESON 1977 Diffusion of carbon dioxide through lipid bilayer membranes. Effects of carbonic anhydrase, bicarbonate,

and unstirred layers. J Gen Physiol 69: 779–794
9. HARNED HS, R DAVIS 1943 The ionization constant of carbonic acid in water and the solubility of carbon dioxide in water and aqueous salt solutions from 0 to 50°. J Am Chem Soc 65: 2030–2037
10. HARNED HS, SR SCHOLES 1941 The ionization constant of HCO_3^- from 0 to 50°. J Am Chem Soc 63: 1706–1709
11. KERN DM 1960 The hydration of carbon dioxide. J Chem Educ 37: 14–23
12. LEHMAN JT 1978 Enhanced transport of inorganic carbon into algal cells and its implication for biological fixation of carbon. J Phycol 14: 33–42
13. LUCAS WJ 1975 Photosynthetic fixation of ^{14}carbon by internodal cells of *Chara corallina*. J Exp Bot 26: 331–346
14. MILLER AG, B COLMAN 1980 Evidence for HCO_3^- transport by the blue-green alga (cyanobacterium) *Coccochloris peniocystis*. Plant Physiol 65: 397–402
15. POCKER Y, DW BJORKQUIST 1977 Stopped-flow studies of carbon dioxide hydration and bicarbonate dehydration in H_2O and D_2O. Acid-base and metal ion catalysis. J Am Chem Soc 99: 6537–6543
16. SIRS JA 1958 Electrometric stopped-flow measurements of rapid reactions in solution. 2. Glass electrode pH measurements. Trans Faraday Soc 54: 207–212
17. STUMM W, JJ MORGAN 1981 Aquatic Chemistry, Ed 2. Wiley, New York, p 127
18. TSUZUKI M, Y SHIRAIWA, S MIYACHI 1980 Role of carbonic anhydrase in photosynthesis in *Chlorella* derived from kinetic analysis of $^{14}CO_2$ fixation. Plant Cell Physiol 21: 677–688
19. VOLOKITA M, A KAPLAN, L REINHOLD 1983 Nature of the rate-limiting step in the supply of inorganic carbon for photosynthesis in isolated *Asparagus* mesophyll cells. Plant Physiol 72: 886–890